

Rapid Virulence Annotation (RVA): Identification of virulence factors using a bacterial genome library and multiple invertebrate hosts

Nicholas R. Waterfield*^{†‡}, Maria Sanchez-Contreras*[†], Ioannis Eleftherianos*, Andrea Dowling[§], Guowei Yang*, Paul Wilkinson*, Julian Parkhill[¶], Nicholas Thomson[¶], Stuart E. Reynolds*, Helge B. Bode^{||}, Steven Dorus*, and Richard H. ffrench-Constant[§]

*Department of Biology and Biochemistry, University of Bath, Bath BA2 7AY, United Kingdom; [§]Department of Biological Sciences, University of Exeter in Cornwall, Penryn TR10 9EZ, United Kingdom; [¶]Pathogen sequencing group, Wellcome Trust Sanger Institute, Cambridge CB10 1SA, United Kingdom; and ^{||}Department of Pharmaceutical Biotechnology, Saarland University, 66123 Saarbrücken, Germany

Edited by Frederick M. Ausubel, Harvard Medical School, Boston, MA, and approved July 25, 2008 (received for review November 23, 2007)

Current sequence databases now contain numerous whole genome sequences of pathogenic bacteria. However, many of the predicted genes lack any functional annotation. We describe an assumption-free approach, Rapid Virulence Annotation (RVA), for the high-throughput parallel screening of genomic libraries against four different taxa: insects, nematodes, amoeba, and mammalian macrophages. These hosts represent different aspects of both the vertebrate and invertebrate immune system. Here, we apply RVA to the emerging human pathogen *Photorhabdus asymbiotica* using "gain of toxicity" assays of recombinant *Escherichia coli* clones. We describe a wealth of potential virulence loci and attribute biological function to several putative genomic islands, which may then be further characterized using conventional molecular techniques. The application of RVA to other pathogen genomes promises to ascribe biological function to otherwise uncharacterized virulence genes.

bacteria | pathogenomics | screening | toxins | entomopathogenic

The growing speed with which the genomes of bacteria can be sequenced is producing an ever expanding knowledge gap between sequence data and its functional annotation. In the case of bacterial pathogens, the identification of virulence factors has typically relied on genetic knock-out and demonstration that virulence is attenuated in a suitable animal model. This approach is not only time consuming and expensive but also, in the case of the use of vertebrate models, ethically debatable. Here, we demonstrate the power of using parallel screens for the identification of virulence genes using three invertebrate infection models and mammalian macrophages in tissue culture, collectively termed Rapid Virulence Annotation (RVA). RVA utility relies upon similarities between the immune responses of vertebrates and invertebrates. The innate immune systems of insects and mammals share many common features, both mechanistically and genetically (1, 2). In addition, much of the basic cellular machinery and pathways that bacterial pathogens can subvert during infection is also well conserved among eukaryotes, presenting common targets. This suggests that virulence mechanisms used by pathogens of mammals may work against invertebrates and vice versa. Indeed, we suggest many virulence strategies evolved initially to combat invertebrates have subsequently been redeployed against vertebrates (3). To test these predictions, we conducted an RVA-based screen on a recently emerging pathogen, *Photorhabdus asymbiotica*, which is a pathogen of both insects and man (4) and causes invasive soft tissue and disseminated bacteraemic infections (5, 6). *Photorhabdus* are members of the Enterobacteriaceae that live in association with soil dwelling entomopathogenic *Heterorhabditid* nematodes and that invade and kill insects. Infective juvenile nematodes seek out and penetrate the insect prey, regurgitating a small number of *Photorhabdus* cells that evade the immune system, kill the insect, and then bio-convert the tissues into more

bacteria. The worm feeds off the bacteria and reproduces until the insect resource is exhausted, whereupon they repackage the bacteria and leave in search of new prey (7). The requirement to overcome the insect immune system and to keep the insect cadaver free of saprophytic organisms in the soil means that all *Photorhabdus* produce a range of bioactive molecules including immune inhibitors, toxins, and powerful antimicrobials. The fully annotated genome sequence of the insect-only pathogen *Photorhabdus luminescens* strain TT01 is available (8) and the genome sequence of the clinical isolate *Photorhabdus asymbiotica* ATCC43949 is almost completed (http://www.sanger.ac.uk/Projects/P_asymbiotica/). The availability of the two genomes allows us to correlate the RVA data with regions unique to the human pathogenic *P. asymbiotica*.

For RVA analysis we sheared the *P. asymbiotica* ATCC43949 genome and cloned it into recombinant *Escherichia coli*. The library, covering 91.4% of the estimated 5.0 Mb genome with an average insert size of 37 kb, was arrayed into 16 96-well plates. All 1,536 clones were sequenced at both ends and end-sequences were assembled onto the genomic scaffold. This cosmid library was screened for gain of toxicity (GOT) assays against the nematode *Caenorhabditis elegans* (nGOT), serving as an oral route model; the single-cell protozoa *Acanthamoeba polyphaga* (aGOT), used as a phagocytosis model; and two caterpillar models (iGOT), the Tobacco hornworm *Manduca sexta* and the Waxmoth *Galleria mellonella*, both of which represent the more complex insect immune systems. Numerous examples of the use of invertebrates as model hosts can be found in the literature (1, 9–12). Finally, we used the mouse BALB/c macrophage cell line J774–2 (mGOT) to represent the phagocytic component of the vertebrate immune system. The use of GOT studies in *E. coli*, in which the model host is challenged with individual clones, has the advantage over chromosomal mutagenesis of "unmasking" any virulence factors that would otherwise be hidden due to toxin redundancy or the presence of potent dominant toxins. To define the virulence-related regions (RVA regions), the end sequences of cosmids showing an effect were assembled onto a

Author contributions: N.R.W. and R.f.-C. designed research; M.S.-C., I.E., A.D., and G.Y. performed research; N.R.W., P.W., J.P., N.T., S.E.R., H.B.B., and S.D. analyzed data; and N.R.W., M.S.-C., and R.f.-C. wrote the paper.

The authors declare no conflict of interest.

This article is a PNAS Direct Submission.

Data deposition: The sequences reported in this paper have been deposited in the EMBL database (accession nos. FM211043–FM211060).

[†]These authors contributed equally.

[‡]To whom correspondence should be addressed. E-mail: bssnw@bath.ac.uk.

This article contains supporting information online at www.pnas.org/cgi/content/full/071114105/DCSupplemental.

© 2008 by The National Academy of Sciences of the USA

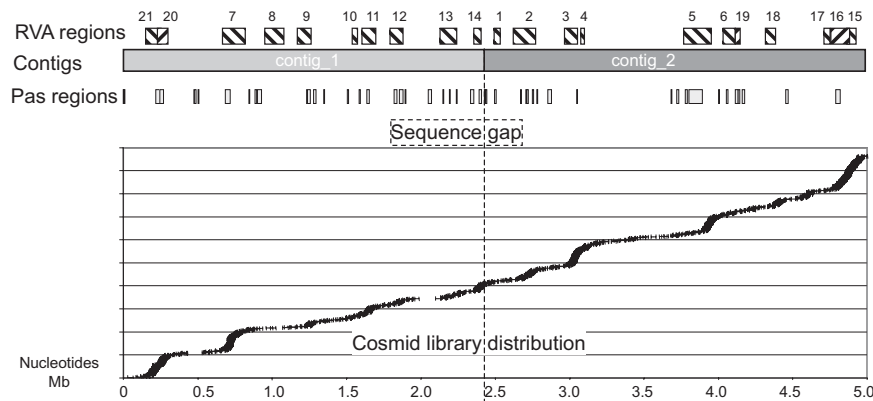


Fig. 1. RVA functional genomics map for *P. asymbiotica*. Boxes on the top layer represent the RVA regions (see Figs. S2–S22). The two large contigs of the *P. asymbiotica* ongoing genome sequencing project are shown. “Pas” regions contain genes that *do not* identify homologues in *P. luminescens* TT01 (at 75% identity level). The lower panel represents the actual genomic locations of the cosmids from the library analyzed by RVA screen. The dotted line represents a sequencing gap, however, the order and orientation of the two large contigs is confirmed by the correct end sequence alignment of five cosmids across this region. Note that a sequence gap of unknown size also exists so the other ends of the contigs are not contiguous.

genomic scaffold and regions of minimum genetic overlap within these clusters were identified, often leading to the identification of specific candidate ORFs or operons. Cross-comparison of genomic regions identified in different assays also gives us an indication of the specificity of the virulence factors identified.

Results

The application of RVA to *P. asymbiotica* gave a high detection rate of candidate gene clusters, encoding virulence factors, which is a reflection of both the sensitivity of RVA method and also the high level of redundancy in encoded pathogenesis factors in *Photorhabdus* bacteria (7, 8, 13). The RVA regions were aligned against the current assembly of the *P. asymbiotica* genome (Fig. 1), each region representing a cluster of cosmids identified either in a single screen (with a minimum of two overlapping cosmids) or via a number of parallel screens in combination (Fig. 2). The complete RVA dataset and more detailed diagrammatic summaries of the 21 RVA regions identified are presented in Table 1 and in supporting information (SI) *Materials and Methods*, Figs. S1–S25, and Tables S1 and S2. Figs. S2–S22 show corre-

lations between gene clusters and the effects on the mammalian and invertebrate model targets. For brevity, here we will only discuss specific examples of the different classes of virulence factors detected, illustrating the robust nature of RVA-based screening.

Re-identification of Known Virulence Factors. The effectiveness of RVA is confirmed by the reidentification of previously known virulence factors, also providing an excellent “internal” positive control. Thus, as anticipated, RVA detected *mcf1* (RVA20) that encodes a dominant insecticidal toxin (14) and also the phage-related toxin delivery system *PVCpnf* (RVA21) (15). Some cosmids containing part or the full *PVCpnf* cluster, detected in iGOT, aGOT, and mGOT assays, also contain a hemagglutinin-like gene. However, one iGOT cosmid (Fig. S22) carries a complete copy of *PVCpnf* along with a truncated nonribosomal peptide synthase (NRPS), indicating that *PVCpnf* alone exhibits toxicity to insects as previously demonstrated (15). Cosmids containing *mcf1* were identified in all types of parallel screens, consistent with the ability of *Mcf1* to cause apoptosis in both insect and mammalian tissues (16). Fig. 2 illustrates how a detailed examination of the cosmid locations relative to the genome can reveal the contribution of different gene clusters to toxicity. In several of the *mcf1*-containing cosmids, the further involvement of tightly linked upstream and downstream NRPS genes in the nGOT and iGOT screens could not be ruled out. Conversely, several cosmids were identified in the mGOT and aGOT assays, which contained only intact *mcf1* and one cosmid from each assay that contained only the downstream NRPS cluster. Cosmid 3AG4, carrying only *mcf1* (identified by aGOT), was tested against the other models resulting in toxic phenotypes, severe feeding delay in the nematodes, insect death at 24 h, and an exhibition of the typical “floppy” phenotype consistent with intoxication by *Mcf1* (14).

Identification of Virulence Factor Homologues. Further confidence in RVA comes from the detection of homologues of virulence factors from other organisms. A “type VI” virulence secretion system described in *Vibrio cholerae* V52 is proposed to provide a target for vaccines and therapeutic agents (17). The *P. asymbiotica* RVA screen identified a highly homologous gene cluster (RVA11) detected in the iGOT assay that is 46–90% similar at the predicted amino acid level (Figs. S12 and S23). Indeed, subsequent work has confirmed the importance of a homologous operon in *Burkholderia mallei* (18). Interestingly, cosmids toxic

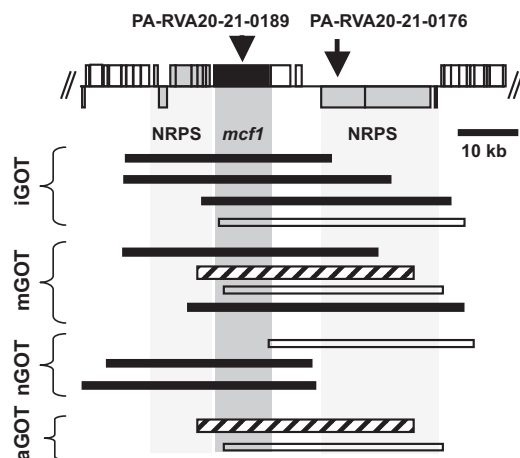


Fig. 2. Biologically active cosmids in the RVA20 region. Boxes above and below the top central line represent ORFs on the forward and reverse strands. RVA positive cosmids are represented below as bars. Hatched bars represent cosmids containing only intact *mcf1*. Black bars represent cosmids containing intact *mcf1* and at least one of the up- or downstream NRPS clusters. Open bars represent cosmids encoding the NRPS downstream of *mcf1* but not the intact gene.

Table 1. Regions of the *P. asymbiotica* ATCC43949 genome identified by RVA analysis

RVA region	Accession number (locus tag range)	Assay	Gene clusters and predicted function
RVA1	FM211043 (PA-RVA1-4467-4422)	iGOT nGOT	Type 3 secretion system genes and <i>exoU</i> effector
RVA2	FM211044 (PA-RVA2-4341-4267)	iGOT mGOT	Hemolysin and PKS modules
RVA3	FM211045 (PA-RVA3-4024-3964)	iGOT mGOT nGOT aGOT	Hemagglutinin-like gene and two NRPS clusters
RVA4	FM211046 (PA-RVA4-3953-3929)	mGOT	<i>xaxAB</i> homologues and hemagglutinin-like gene
RVA5	FM211047 (PA-RVA5-3244-3168)	iGOT mGOT nGOT aGOT	<i>PVClumt</i> , <i>evp</i> operon and hemagglutinin
RVA6	FM211048 (PA-RVA6-3081-3019)	iGOT nGOT	Fimbrial operon and Pdl-GI-1 island
RVA7	FM211049 (PA-RVA7-0626-0673)	iGOT mGOT nGOT aGOT	Invasin and unknown genes
RVA8	FM211050 (PA-RVA8-2849-2974)	nGOT	Unknown
RVA9	FM211051 (PA-RVA9-1890-1949)	iGOT mGOT aGOT	Prophage
RVA10	FM211052 (PA-RVA10-2214-2246)	mGOT aGOT	Fimbrial operon
RVA11	FM211053 (PA-RVA11-2280-2352)	iGOT mGOT nGOT aGOT	Hemagglutinin and type VI secretion system
RVA12	FM211054 (PA-RVA12-2456-2515)	nGOT mGOT	Unknown
RVA13	FM211055 (PA-RVA13-1315-1206)	iGOT nGOT mGOT	Pdl-GI-4 and <i>ast</i> enterotoxin homologue
RVA14	FM211056 (PA-RVA14-1110-1068)	iGOT aGOT	Hemagglutinin-like and NRPS cluster
RVA15	FM211057 (PA-RVA15_17-0915-0951)	iGOT aGOT	<i>rtxA</i> homologue, NRPS and <i>evp</i> -like operon
RVA16	FM211057 (PA-RVA15_17-0915-0992)	iGOT mGOT nGOT aGOT	<i>vgrG</i> , <i>rtxA</i> homologues and NRPS
RVA17	FM211057 (PA-RVA15_17-1004-1042)	iGOT nGOT mGOT	<i>kdp</i> operon and a perforin-like gene
RVA18	FM211058 (PA-RVA18-1596-1632)	iGOT mGOT	NRPS and PKS-like gene clusters
RVA19	FM211059 (PA-RVA19-1780-1813)	iGOT	Pdl-GI-2 and putative virulence factor <i>mvnI</i>
RVA20	FM211060 (PA-RVA20_21-0210-0176)	iGOT mGOT nGOT aGOT	Two NRPS clusters and <i>mcf1</i> cytotoxin
RVA21	FM211060 (PA-RVA20_21-0176-0072)	iGOT mGOT aGOT	<i>PVCpnf</i> and hemagglutinin-like gene

Illustrations of this information can be seen in Figs. S2–S22. Full annotation of these regions can be found in the EMBL entries indicated by accession numbers.

to macrophages (mGOT) also span an adjacent region that contains the putative *vgrG* toxin unique to the human pathogen *P. asymbiotica* and absent from *P. luminescens*, potentially representing a genomic island specialized for mammalian pathogenicity. Further, an RVA region showing activity in all assays (locus tag PA-RVA5-3205 to 3199, Fig. S6) is homologous (48–72% similar at the amino acid level) to the type-VI like *evp* operon involved in virulence in the fish pathogen *Edwardsiella tarda* (19, 20).

Functional Annotation of Secondary Metabolite Gene Clusters. It is notoriously difficult to ascribe biological function to gene clusters responsible for the synthesis of secondary metabolites such as polyketide synthesis (PKS) and non-ribosomal peptide synthesis (NRPS) enzyme complexes. Like many pathogens, *Photobacterium* dedicates a large amount of coding sequence to the manufacture of small molecules but their biological roles and structures remain unknown. RVA identified a number of regions predicted to encode NRPS/PKS-like complexes and Fig. 3A illustrates four examples of identified cosmids that exhibit a range of activities including the ability of the recombinant *E. coli* to kill *G. mellonella* upon injection (Fig. 3B). HPLC/MS analysis of preparations from cosmids 4DB5 (RVA5) and 1DF9 (RVA14) identified 265.4/468.4 and 586.4 as specific $[M+H]^+$ masses for the respective molecules, which were not present in the *E. coli* control (Fig. S24). Two compounds were identified from cosmid 4DB5 (RVA5) encoding a gene cluster with high similarity to the yersiniabactin biosynthesis genes. The postulated sum formula $C_{12}H_{12}ON_2S_2$ is identical to the sum formula of ulbactin E, a short derivative of yersiniabactin, which has been described from a marine *Alteromonas* strain (21). The second compound $C_{20}H_{25}O_4N_3S_3$ might represent a desmethyl-derivative of yersiniabactin ($C_{21}H_{27}O_4N_3S_3$) that has not been described in the literature yet. The identified sum formula of $C_{32}H_{51}O_5N_5$, from 1DF9 cosmid (RVA14), fits well with the structure of a cyclic pentapeptide. Interestingly, an identical sum formula is found in sansalvamide A peptides (22–24), synthetic derivatives of the depsipeptide natural product sansalvamide A that were isolated from a marine fungus and showed potent anti-cancer activity (25). Isolation of all identified compounds

for detailed structure elucidation is currently underway. Preliminary structural predictions of other secondary metabolites identified by RVA are presented in Table S1. One example is the predicted compound encoded by RVA 18 (Fig. S19) similar to a new antitumor antibiotic: glidobactin from *Polyangium brachysporum* (26). Two PKS clusters and one NRPS gene cluster were also encoded in mGOT RVA regions, suggesting that secondary metabolites produced from these operons could have potential roles in human pathogenicity. The rapid identification of new biological activities from these secondary metabolite synthetic genes suggests that RVA analysis can be a powerful method of drug discovery.

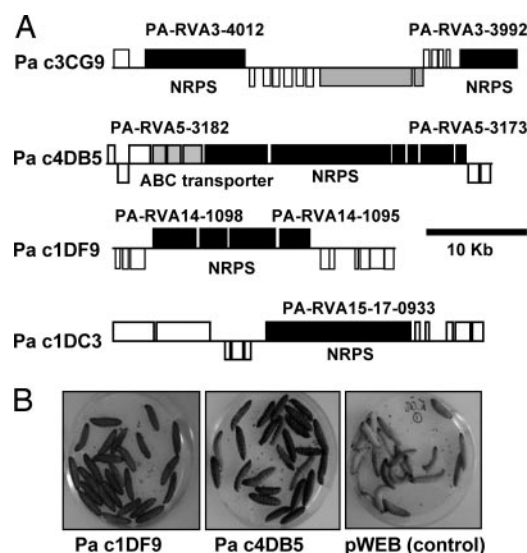


Fig. 3. Functional NRPS gene clusters identified by RVA. (A) Gene maps of four cosmids encoding NRPS genes that were identified using RVA screens. Boxes above and below the lines represent ORFs on the forward and reverse strands respectively. (B) Two of these cosmids showed toxicity to *G. mellonella* compared with the control (pWEB vector).

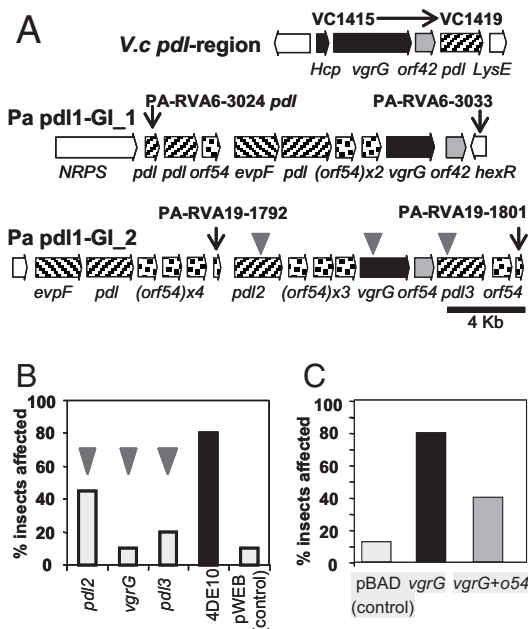


Fig. 4. Putative novel virulence factors detected by RVA. (A) Comparison of a *pdl* operon in *Vibrio cholerae* O1 strain N16961 (Top) and two of the four *pdl*-*o54* islands of *P. asymbiotica* ATCC43949. Homologous genes are coded by shading. Gray triangles represent transposon insertions in three individual genes for fine-scale mapping (see below). (B) Fine-scale mapping of the *Pa pdl1-GL2* virulence island. The insertion mutants of the two *pdl* genes and the *vgrG* gene all show reduced toxicity when injected to *G. mellonella*, while the wild-type cosmid (4DE10) is fully toxic. Injection of control *E. coli* (pWEB cosmid) had negligible effect. (C) The *vgrG* toxin with or without the small flanking *orf54* were cloned into the arabinose-inducible expression vector pBAD30. When induced, these clones were toxic by injection to *G. mellonella*. Interestingly, cloned *orf54* reduced this effect suggesting its function is antagonistic to the toxic phenotype.

Identification of Virulence Gene Clusters. Our recent work on secretion of the orally active Toxin Complex d (Tcd) from *P. luminescens* indicates that a putative class III lipase *pdl* (27) is responsible for release of Tcd from the outer membrane of the bacterium and that this process is negatively regulated by the tightly linked gene *orf54* (G. Yang and N.R.W., unpublished work). We detected several regions encoding *pdl*-*o54* gene homologues in the *P. asymbiotica* genome that were toxic to either insects and/or nematodes. We therefore speculate that these represent virulence loci (Fig. 4A, and Figs. S7 and S20). We note that these regions have no effect on the mammalian macrophages again suggesting some specificity in their toxicity. Interestingly, *pdl*-islands are also present in the genomes of many other Gram-negative pathogens, including *Vibrio cholerae*, suggesting they also may be virulence determinants in other human pathogens. In characterizing RVA regions such as these, determination of the minimal region of overlap between “toxic” cosmids at any given locus may not provide sufficient clues to suggest the exact genes responsible. Thus, we carried out insertional mutagenesis to map the genes causing the phenotype by using an *in vitro* mutagenesis kit to construct insertion mutant libraries of toxic cosmids. Clones with insertions in different genes are then identified by sequencing out from the integrated transposon. The mutated cosmids are rescreened in the appropriate RVA assay to identify clones showing loss of function and therefore the ORF responsible. In the case of the *Pa pdl1-GL2* insecticidal region, we selected the 4DE10 toxic cosmid for this fine-scale mapping (Fig. 4B). This identified *vgrG* and two of the *pdl*-homologues as necessary for the toxic effect on *G. mellonella*. Subcloning and heterologous expression of *vgrG* in *E. coli* (Fig.

4C) confirmed the toxicity of this gene product and serves to illustrate how RVA allows us to move from a whole genome to an individual toxin gene with ease.

Importantly, the RVA approach is also powerful in identifying genes with functions that could not be predicted using conventional genetic approaches. Three cosmids were identified in the iGOT screen, 3CD1, 3DB8, and 1AA3 (RVA17, Fig. S18), causing a moribund phenotype when injected to *M. sexta*. Fine-scale mapping traced the toxic effect to *kdpEDCBAF* encoding the high affinity potassium pump (28) of *P. asymbiotica* (Fig. S25). Over-expression of the Kdp pump appears to allow the bacteria to persist and even grow in the hemocytes (I. Vlisidou and N.R.W., unpublished work). This striking fundamental discovery is likely to be relevant to all immune cell-pathogen interactions, which rely upon high potassium gradients for maturation of the phagolysosome (29). We propose that the assumption-free RVA screening technology is ideal for making such discoveries and expect many more from a range of pathogens.

Virulence Against Insect or Man? It was anticipated that in the case of *P. asymbiotica*, a comparison between the invertebrate and macrophage (mGOT) RVA data could provide candidate genes responsible for facilitating human infection. Cosmids in RVA4 were identified by the mGOT screen but not in either of the invertebrate assays. This region does not encode genes unique to the human pathogenic *P. asymbiotica* and, therefore, has homologues in the insect-only pathogen *P. luminescens* TT01. RVA4 (Fig. S5) contains homologues of the proapoptotic *xaxAB* from *Xenorhabdus* (30) and a large hemolysin/hemagglutinin gene, either of which may represent potential virulence factors. Interestingly, the majority of mGOT regions are also shown to have effects in invertebrate hosts, supporting our hypothesis that genes evolved to combat invertebrates can be redeployed against mammalian hosts (3).

Discussion

Here, we have demonstrated the ability of RVA to identify virulence loci via the parallel screening of a recombinant DNA library in a non-pathogenic laboratory strain of *E. coli* against a range of different taxa. The RVA analysis of *P. asymbiotica* identified a range of different putative virulence factors including eight NRPS operons, two PKS operons, six hemolysin/hemagglutinin-like genes, three pili/fimbrial operons, seven putative specialized secretion systems (PVC*pnf*, T6SS, Evp-islands, T3SS and Pld-islands) and at least seven toxin-like genes (homologues of *mcf1*, *xaxAB*, *vgrG*, *rtxA*, *xnt2*, *ast*, and a VIP2 family gene). The identification of such a large number of virulence loci illustrates that RVA is useful as a means of generating preliminary biological annotation relating to pathogenic phenotypes. RVA annotation highlights operons or genes as potentially important in virulence that can then be investigated in greater detail either for accurate annotation or more specific applications (i.e., drug discovery or vaccine candidates). Therefore, fine-scale mapping of RVA regions, by transposon mutagenesis or cloning individual ORFs, is essential to confirm the exact genes responsible for toxicity in each cluster. The use of different invertebrate targets with less complex immune responses (insects, nematodes, and protozoa) allows the detection of less “potent” virulence factors that could otherwise be overlooked in whole animal mammalian models. It is interesting that most of the virulence factors identified in the mGOT assay were also toxic in the invertebrate screens confirming the general utility of invertebrates as model hosts for disease studies. Although it is likely that a small subset of host-specific virulence factors will not be detected by RVA, the screens are nevertheless sensitive enough to detect a very large number of more numerous general virulence factors.

The power of the RVA technique relies on several factors. First and highly important is the coverage and the depth of the

genomic library used that covered >90% of the genome, with nearly 80% being covered by two or more clones. The analysis of the cosmid library distribution on the genome assembly confirmed that some regions are more represented than others and certain regions are absent. In future RVA studies it may be pertinent to “normalize” the library by selecting a subset of cosmids for the assays, reducing the level of redundancy in testing while still maximizing genome coverage. The second factor is the underlying genetic architecture of virulence factors. RVA’s strength is in the identification of single-loci virulence factors and multilocus virulence factors that are tightly clustered within a bacterial genome. Molecular characterization of virulence factors to date suggests that the majority fall into these categories, further justifying our screening approach. However, there are several notable examples of virulence factors for which the underlying genetics basis is complex and involves multiple genes or regions of the genome, and these will naturally not be identified by RVA. This limitation can be overcome by using vectors that accommodate larger fragments such as BACs.

Frequent concerns regarding heterologous expression in *E. coli* include potential problems in differing G+C content between host and donor DNA and a failure of *E. coli* expression machinery either to recognize the donor gene expression signals or to provide the appropriate secretion machinery. Nevertheless, the successful application of RVA to *Photorhabdus*, with an average G+C content of 42%, significantly lower than the 50% of *E. coli*, indicates that this is not a current limitation to these biological screens. One reason why *E. coli*-based expression is more successful than expected may relate to the fact that pathogenicity islands that have been recently horizontally acquired may be more prone to gene expression in differing host backgrounds, and indeed this may actually be a requirement of such elements if they are to be positively selected in nature. Furthermore, the RVA technique does not only rely on correct secretion of the heterologously expressed virulence factors as whole cultures are used in the screens. We note that cytoplasmically accumulated toxins can be detected in these assays, as demonstrated by the insect toxicity of *E. coli* expressing but not secreting the Mef1 toxin (14). The application of RVA to more diverse bacterial pathogens will ultimately define the limits of its utility, although in principle the host strain used need not be *E. coli* and libraries from Gram-positive pathogens could be screened in different host species (such as *Lactococcus*).

We believe that RVA represents an excellent way to provide basic information about general virulence determinants in poorly understood pathogens and to add functional relevance to the ongoing annotation of pathogen genome sequences. It also provides an alternative strategy for virulence gene detection across whole genomes, important for current efforts toward the reduction and replacement of animal testing.

Materials and Methods

Cosmid Library Construction and Statistical Analysis. The *P. asymbiotica* ATCC43949 genomic library was constructed in the pWEB vector (Epicentre) in *E. coli* EP1305™ by MWG Biotech. The 1,536 resulting cosmids were arrayed into 16 96-well plates and end-sequenced before storage at –80 °C. Cosmid size and location were determined by BLASTN comparison of each end against the unfinished genome. Average cosmid length is 37,014 bp (SD = 4578.4) and 4,605,359 bp is covered representing 91.4% of the estimated 5.0 Mb genome.

Average fold coverage is >7 fold and 79.75% of genome has twofold coverage or more. There are 17 gaps with a relatively large average gap size of 25,602bp (SD = 32,568) due to 2 large gaps while the remainder are smaller, typically <1000bp. Library plates were subcultured in LB medium supplemented with 100 µg/ml ampicillin and/or 50 µg/ml kanamycin. Transposon mutagenesis was done using the EZ-Tn5<Tet> kit (Epicentre).

Invertebrates Maintenance. *M. sexta* were reared in controlled conditions (25 °C, 80% humidity) on artificial diet (31) and fifth instar larvae were used for iGOT. *G. mellonella* was purchased from Livefood Ltd for fine-scale mapping analysis. *C. elegans* were raised at 18 °C on NGM medium (32) using *E. coli* OP50 as feeding strain and transferred weekly to fresh plates. Adult worms were washed off plates with Phosphate Saline Buffer and the suspension adjusted to 10 nematodes per 10 µl drop. *A. polyphaga* was grown in PYG medium (33) at 25 °C, and subcultured weekly. Stationary phase (5 days) cultures were used for aGOT, adjusting the number of cells to 2×10^5 cells/ml using a haemocytometer.

Gain of Toxicity Assays (GOT). 100 µl of overnight cosmid cultures were injected into individual *M. sexta* larvae that were scored for death or severe delay in development daily during one week. Every cosmid showing an effect was retested on a further 10 insects allowing confirmation of the phenotype. For nGOT/aGOT, a 10 µl drop of overnight culture from each individual cosmid was grown on 25-well plates containing NGM agar with 50 µg/ml ampicillin (nGOT) or PYG agar with 50 µg/ml kanamycin (aGOT). The plates were inoculated with 10 µl of the adjusted suspensions of *C. elegans* or *A. polyphaga* respectively and incubated at 22 °C for 7 days. Toxicity was assessed both by eye and under an inverted microscope and avoidance or delay in feeding was scored using an arbitrary scale of 0 to 5 (5 being no consumption, 3 half-consumed and 0 completely consumed). For mGOT, the mouse BALB/c monocyte macrophage cell line J774–2 was seeded at 1×10^3 cells per ml into 96-well plates, in Dulbeccos Modified Eagles Medium (DMEM) supplemented with 10% fetal bovine serum, 5% non-essential amino acids, and 100 µg/ml ampicillin and incubated overnight (37 °C, 5% CO₂). Cosmid cultures were harvested by centrifugation and cells subjected to lysozyme treatment followed by freeze-thaw cycles. Crude lysates were applied to the macrophage plates and incubated for 24 h. Subsequently, the mix was aspirated from the macrophages and replaced with phenol red-free DMEM, with 2% 100X solution penicillin/streptomycin and 50 µg/ml gentamicin and incubated under the same conditions for 2 h. Cell viability was ascertained using the XTT assay (34). Candidate cosmid clones were selected for their ability to reduce cell viability by 40% comparative to untreated cells.

HPLC/MS Analyses and Secondary Metabolite Structure Prediction. Cosmids 4DB5 and 1DF9 were coexpressed in *E. coli* EC100 with pSUMtaA (35), which encodes a promiscuous phosphopantetheine transferase from *Stigmatella aurantiaca* DW4/3–1. After three days of growth in LB medium with 2% Amberlite XAD-16 adsorber resin (Fluka), the resin was harvested by centrifugation and extracted with 10 ml of MeOH. The organic extract was evaporated to dryness, dissolved in 1 ml of MeOH, centrifuged to get rid of solid material, and finally analyzed by HPLC/MS as described in ref. 36. Sum formulas were determined from the masses after HR-MS using a LTQ-Orbitrap Hybrid MS (Thermo) and databases searches were performed with the obtained predictions. The annotation of gene clusters putatively involved in secondary metabolite production was done by analyzing the protein sequences with a program written by Jacques Ravel (University of Maryland School of Medicine, Baltimore, MD) for overall domain organization and the NRPS predictor for adenylation specificity of the NRPS adenylation domains (37). In cases where no functional assignments could be made for full proteins or parts thereof, a BLASTP analysis was performed.

ACKNOWLEDGMENTS. We thank Sandra Barns for the maintenance of *M. sexta* and *C. elegans*, and Sharon Huws for *A. polyphaga* gift. This work was funded by the BBSRC.

- Khush RS, Lemaitre B (2000) Genes that fight infection: What the *Drosophila* genome says about animal immunity. *Trends Genet* 16:442–449.
- Sadd BM, Schmid-Hempel P (2006) Insect immunity shows specificity in protection upon secondary pathogen exposure. *Curr Biol* 16:1206–1210.
- Waterfield NR, Wren BW, Ffrench-Constant RH (2004) Invertebrates as a source of emerging human pathogens. *Nat Rev Microbiol* 2:833–841.
- Gerrard J, Waterfield N, Vohra R, Ffrench-Constant R (2004) Human infection with *Photorhabdus asymbiotica*: An emerging bacterial pathogen. *Microbes Infect* 6:229–237.
- Farmer JJ, et al. (1989) *Xenorhabdus luminescens* (DNA hybridization group 5) from human clinical specimens. *J Clin Microbiol* 27:1594–1600.
- Gerrard JG, Joyce et al. (2006) Nematode symbiont for *Photorhabdus asymbiotica*. *Emerg Infect Dis* 12:1562–1564.
- Ffrench-Constant R, et al. (2003) *Photorhabdus*: Towards a functional genomic analysis of a symbiont and pathogen. *FEMS Microbiol Rev* 26:433–456.
- Duchaud E, et al. (2003) The genome sequence of the entomopathogenic bacterium *Photorhabdus luminescens*. *Nat Biotechnol* 21:1307–1313.
- Sifri CD, Begun J, Ausubel FM (2005) The worm has turned—microbial virulence modeled in *Caenorhabditis elegans*. *Trends Microbiol* 13:119–127.
- Kaito C, et al. (2005) Silkworm pathogenic bacteria infection model for identification of novel virulence genes. *Mol Microbiol* 56:934–944.

11. Lauriano CM, et al. (2004) MglA regulates transcription of virulence factors necessary for *Francisella tularensis* intraamoebae and intramacrophage survival. *Proc Natl Acad Sci USA* 101:4246–4249.
12. Molmeret M, Horn M, Wagner M, Santic M, Abu Kwaik Y (2005) Amoebae as training grounds for intracellular bacterial pathogens. *Appl Environ Microbiol* 71:20–28.
13. ffrench-Constant RH, et al. (2000) A genomic sample sequence of the entomopathogenic bacterium *Photorhabdus luminescens* W14: Potential implications for virulence. *Appl Environ Microbiol* 66:3310–3329.
14. Daborn PJ, et al. (2002) A single *Photorhabdus* gene makes caterpillars floppy (*mcf*) allows *Escherichia coli* to persist within and kill insects. *Proc Natl Acad Sci USA* 99:10742–10747.
15. Yang G, Dowling AJ, Gerike U, ffrench-Constant RH, Waterfield NR (2006) *Photorhabdus* virulence cassettes confer injectable insecticidal activity against the wax moth. *J Bacteriol* 188:2254–2261.
16. Dowling AJ, et al. (2004) The insecticidal toxin makes caterpillars floppy (*Mcf*) promotes apoptosis in mammalian cells. *Cell Microbiol* 6:345–353.
17. Pukatzki S, et al. (2006) Identification of a conserved bacterial protein secretion system in *Vibrio cholerae* using the *Dictyostelium* host model system. *Proc Natl Acad Sci USA* 103:1528–1533.
18. Schell MA, et al. (2007) Type VI secretion is a major virulence determinant in *Burkholderia mallei*. *Mol Microbiol* 64:1466–1485.
19. Rao PS, Yamada Y, Tan YP, Leung KY (2004) Use of proteomics to identify novel virulence determinants that are required for *Edwardsiella tarda* pathogenesis. *Mol Microbiol* 53:573–586.
20. Zheng J, Leung KY (2007) Dissection of a type VI secretion system in *Edwardsiella tarda*. *Mol Microbiol* 66:1192–1206.
21. Kikuchi K, et al. (1998) New alkaloids, ulbactins D and E, and their manufacture with *Alteromonas*. *Jpn. Kokai Tokkyo Koho*, 6 pp. CODEN: JKXXAF JP 10245377 A 19980914 Heisei. CAN 129:244217 AN 1998:600005 CAPLUS.
22. Gu WX, Liu SX, Silverman RB (2002) Solid-phase, Pd-catalyzed silicon-aryl carbon bond formation. Synthesis of sansalvamide A peptide. *Org Lett* 4:4171–4174.
23. Carroll CL, et al. (2005) Synthesis and cytotoxicity of novel sansalvamide A derivatives. *Org Lett* 7:3481–3484.
24. Otrubova K, Lushington G, Velde DV, McGuiere KL, McAlpine SR (2008) Comprehensive study of sansalvamide derivatives and their structure-activity relationships against drug-resistant colon cancer cell lines. *J Med Chem* 51:530–544.
25. Belofsky GN, Jensen PR, Fenical W (1999) Sansalvamide: A new cytotoxic cyclic depsipeptide produced by a marine fungus of the genus *Fusarium*. *Tetrahedron Lett* 40:2913–2916.
26. Schellenberg B, Bigler L, Dudler R (2007) Identification of genes involved in the biosynthesis of the cytotoxic compound glidobactin from a soil bacterium. *Environ Microbiol* 9:1640–1650.
27. Waterfield NR, Daborn PJ, ffrench-Constant RH (2004) Insect pathogenicity islands in the insect pathogenic bacterium *Photorhabdus*. *Physiological Entomology* 29:1–11.
28. Walderhaug MO, et al. (1992) KdpD and KdpE, proteins that control expression of the *kdpABC* operon, are members of the two-component sensor-effector class of regulators. *J Bacteriol* 174:2152–2159.
29. Reeves EP, et al. (2002) Killing activity of neutrophils is mediated through activation of proteases by K⁺ flux. *Nature* 416:291–297.
30. Vigneux F, et al. (2007) The *xaxAB* genes encoding a new apoptotic toxin from the insect pathogen *Xenorhabdus nematophila* are present in plant and human pathogens. *J Biol Chem* 282:9571–9580.
31. Reynolds SE, Nottingham SF, Stephens AE (1985) Food and water economy and its relation to growth in 5th-instar larvae of the Tobacco Hornworm, *Manduca sexta*. *J Insect Physiol* 31:119–127.
32. Stiernagle T (2006) Maintenance of *C. elegans*. *Wormbook*. Available at <http://www.wormbook.org>. Accessed July 23, 2008.
33. Rowbotham TJ (1980) Preliminary report on the pathogenicity of *Legionella pneumophila* for freshwater and soil amoebae. *J Clin Pathol* 33:1179–1183.
34. Scudiero DA, et al. (1988) Evaluation of a soluble tetrazolium/formazan assay for cell growth and drug sensitivity in culture using human and other tumor cell lines. *Cancer Res* 48:4827–4833.
35. Gaitatzis N, Hans A, Muller R, Beyer S (2001) The *mtaA* gene of the myxothiazol biosynthetic gene cluster from *Stigmatella aurantiaca* DW4/3–1 encodes a phosphopantetheinyl transferase that activates polyketide synthases and polypeptide synthetases. *J Biochem* 129:119–124.
36. Brachmann AO, Forst S, Furgani GM, Fodor A, Bode HB (2006) Xenofuranones A and B: Phenylpyruvate dimers from *Xenorhabdus szentirmaii*. *J Nat Prod* 69:1830–1832.
37. Rausch C, Weber T, Kohlbacher O, Wohleben W, Huson DH (2005) Specificity prediction of adenylation domains in nonribosomal peptide synthetases (NRPS) using transductive support vector machines (TSVMs). *Nucleic Acids Res* 33:5799–5808.